ESAT Three-Axis ADCS Implementation

K.S. Olfe*, MSc in Aeronautical Engineering
Escuela Técnica Superior de Ingeniería Aeronáutica y del Espacio,
Universidad Politécnica de Madrid, Plaza Cardenal Cisneros 3, 28040 Madrid, Spain

The general purpose of this work is to develop an optimal three-axis Attitude Determination and Control Subsystem (ADCS) for the satellite ESAT. ESAT is an educational nanosatellite based on the CubeSat standard. This work includes: sensors signal conditioning, 4 implementations of attitude determination algorithms, a Proportional Integrative Derivative (PID) attitude controller, a detumbling controller and the experimental results obtained in low-cost self-designed test-bed. The results obtained show the functional status of the 3-axis ADCS of ESAT which is now an adequate tool to research in the field of satellites attitude control.

I. Introduction

ESAT is an educational satellite designed for hands-on learning for all education levels. It is a 10x10x10cm nanosatellite based on the successful CubeSat standard [1], weighing less than 1kg and having the following typical spacecraft subsystems: Electrical Power, Command and Data Handling, 1-axis Attitude Determination and Control and structure [2]. So, the main purpose of this work is to migrate the ADCS of ESAT from 1-axis controlled to 3-axis controlled. It means that new sensors and actuators have to be used, new determination algorithms and control laws have to be implemented and new telemetry and commands packages have to be send.

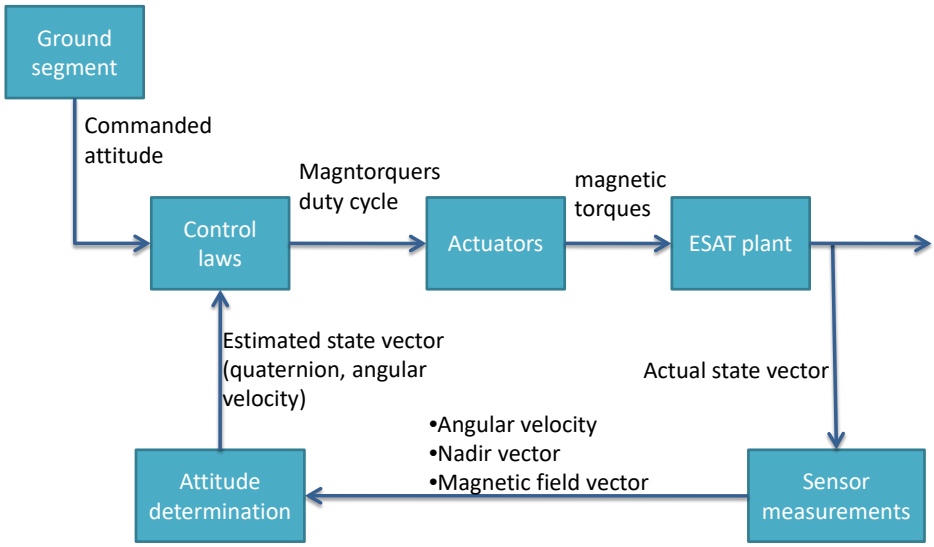

Figure 1. Project Schema

The development of a 3-axis ADCS for the educational satellite ESAT can be seen from a general control design point of view as it is represented in Fig. 1. The controlled plant is the ESAT, its state vector is the controlled variable and includes its orientation as a rigid solid in space and also its angular velocity. To know this vector, there are necessary some measurements which come from on board sensors. These measurements are combined with an attitude determination algorithm which provides an estimation of the current state of the plant. From ground

*kolfe@eusoc.upm.es

segment, a reference state is commanded and the control laws feed the actuators to change the current state of ESAT to desired state (the reference).

During the develop of the 3-axis ADCS for ESAT, a new prototype was used (see Fig. 2) to test both software and hardware described in this document. Tests mentioned in this documents and experimental results exposed were obtained with this prototype. This prototype does not include solar panels, sun sensors and the reaction wheel. It is a magnetic control based concept where a new air core magnetorquer was manufactured and included to generated a dipolar moment component in Z-axis.

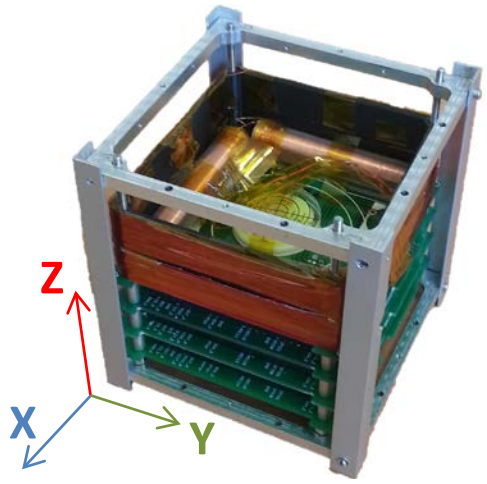

Figure 2. Three-axis controlled ESAT prototype with the body frame reference.

II. Sensors measurements

ESAT is equipped with three-axis gyroscope, accelerometer and magnetometer. All of them are used to determine the attitude and, for that reason, they need to be treated as follows:

Gyroscope signals are filtered with a Digital Low Pass Filter (DLPF) to reduce the high-frequency noise. It is necessary not only to integrate its measurements but also to use this signal as the derivative input of an attitude PID controller.

Since the 3-axis controlled ESAT prototype is not equipped with suns sensors (which determines 2 Degrees of Freedom, DoF), the magnetometer, alone (2 DoF), is unable to get a complete attitude determination (at least 3 DoF). The use of accelerometer as nadir sensor resolves this uncertainty without loss of generality.

III. Attitude Determination

The most common way to represent the attitude of a rigid body is a set of three Euler angles (see Fig. 3). The main disadvantages of Euler angles are that they have singularities and a higher computational cost (due to the trigonometric functions). Any finite rotation may be also achieved by a single rotation about an appropriately chosen axis. It is therefore possible to parameterize the attitude of a rigid body with an angle δ and a unit vector $\vec{\upsilon}$ [3].

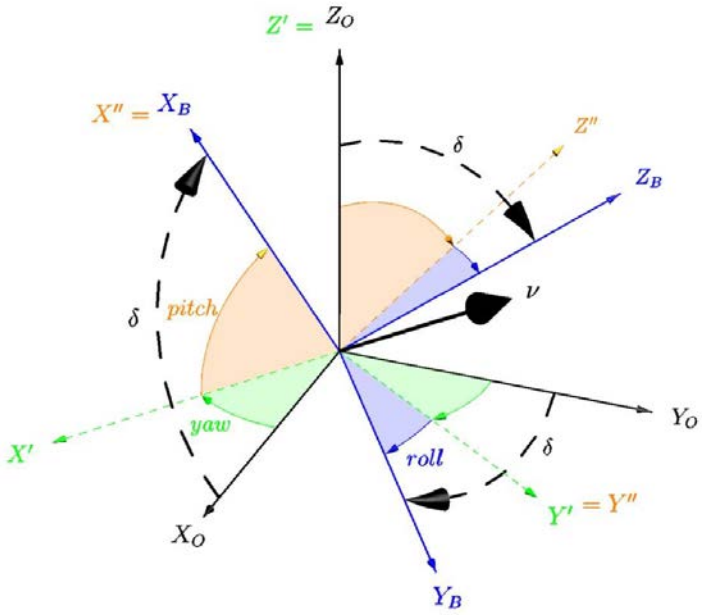

Figure 3. Euler angles and axis-angle representation [3]

ESAT attitude is parametrized in unit quaternions [4,5] whose relation with the axis-angle representation is described in Eq. (1).

$$\vec{q} = \begin{bmatrix} q_1 \\ q_2 \\ q_3 \\ q_4 \end{bmatrix} = \begin{bmatrix} q \\ q_4 \end{bmatrix} = \begin{bmatrix} \sin\left(\frac{\delta}{2}\right)\vec{\upsilon} \\ \cos\left(\frac{\delta}{2}\right) \end{bmatrix} \tag{1}$$

Three different attitude determination algorithms have been implemented in ESAT:

- TRIAD.
- Gyroscope measurements integration.
- Q-method (implemented in two ways).

As it was explained in section II, to completely determine the attitude, the knowledge of the values of at least two vectors both in body frame (see Fig. 2) and in inertial frame is needed because one vector only determine 2 DoF and it is necessary to know 3. With 2 vector, there are 4 DoF restricted and owing to the sensors noise, they will not be consistent (the problem has only 3 DoF so, if there are 4, one should be dependent of the others). TRIAD method solves this inconsistency in a deterministic way, i.e. the same input of the measurements of two vectors generates the same output. Thus, this method does not need any initial attitude approach and it can be used to initialize other methods and to compare the results obtained with other algorithms. In ESAT, this method has been implemented with the measurements of the accelerometer and the magnetometer (in this order).

There are some mission phases where there are no readings from two different vectors, e.g., a mission using a sun sensor during an eclipse phase. To simulate these cases, an algorithm based on the integration of gyroscopes has been also implemented. This implementation allows to deal with the fact that integrating a Gaussian noise during a large amount of time can produce an error in the actual value. Even if the noise has any error in the mean, i.e. the measurements are most probably in the actual value (without any offset error), the final value obtained by the integration of gyroscope signal could be very far to the actual. This is a real problem for satellites and thus, the quaternion value has to be updated with other method when it is possible.

Q-method holds on the definition of a cost function to be minimized. This function (J) has the following structure:

$$J(R) = \frac{1}{2}\sum_{i=1}^{N} a_i \left| \vec{W}_i - R\vec{V}_i \right|^2 \tag{2}$$

Where N is the number of vectors used in the method, W_i are the vectors measured in body frame (see Fig. 2), V_i are the same vectors in inertial frame, R is the rotation matrix and a_i are weight factors. The objective is to found a rotation matrix which minimizes this function, i.e. the attitude which minimizes the squares residuals between the on board measured values and the calculated inertial values. So this method allows to include as many measurements as desired, so it is possible to take into account all the sensors. To compare the attitude obtained with this method with the one obtained with TRIAD, an implementation with only the accelerometer and the magnetometer has been also performed. By writing this problem in terms of quaternios, we derive the following eigenvalue problem:

$$K\vec{q} = \lambda\vec{q} \tag{3}$$

where the matrix K depends on the vectors in the inertial and body frames and the weigtht factors. Since only the largest eigenvalue is required, when the matrix is well conditioned, we solve Eq. (3) by means of the power method described below.

A. Power Method

The power method [6] is a very simply algorithm to obtained the largest eigenvalue (and eigenvector). It consists on recursively multiplying an initial approach to the eigenvector by the matrix (in this case an initial quaternion by the matrix *K*). To avoid numerical problems in each step the quaternion is normalize:

$$\vec{q}_i = K\frac{\vec{q}_{i-1}}{\left|\vec{q}_{i-1}\right|} \tag{4}$$

This step is repeated until the quaternion accomplishes a stop condition which will condition the error of the method.

B. Convergence of power method

The output of the power method (without normalizing the quaternion) in i^{th} step is:

$$\vec{q}_i = K\vec{q}_{i-1} = K^i\vec{q}_0 \tag{5}$$

Where $\vec{q}_0$ is the initial value which begins the iteration. If $\vec{x}_i$ (i = 1; 2; 3; 4) are the eigenvectors of the matrix *K*, the initial value can be expressed as a lineal combination of this vectors:

$$\vec{q}_0 = c_1\vec{x}_1 + c_2\vec{x}_2 + c_3\vec{x}_3 + c_4\vec{x}_4 \tag{6}$$

Where c_i (i = 1; 2; 3; 4) are constant values. Then the output of the i^{th} iteration can be expressed as:

$$\vec{q}_i = K^i\vec{q}_0 = \sum_{j=1}^{4} c_j K^i\vec{x}_j = \sum_{j=1}^{4} c_j\lambda_j^i\vec{x}_j = \lambda_1^i\left[c_1\vec{x}_1 + \sum_{j=2}^{4} c_j\left(\frac{\lambda_j}{\lambda_1}\right)^i\vec{x}_j\right] \tag{7}$$

Where λ_j (j = 1; 2; 3; 4) are the eigenvalues ordering such that:

$$\left|\lambda_1\right| > \left|\lambda_2\right| > \left|\lambda_3\right| > \left|\lambda_4\right| \tag{8}$$

For this reason the coefficients of $\vec{x}_j$ (j = 2; 3; 4) converge to zero as $i \to \infty$. Note that if $\left|\lambda_1\right| > 1$ the vector $\vec{q}_i$ increases its norm in each iteration. In the opposite, if $\left|\lambda_1\right| < 1$, $\left\|\vec{q}\right\|_i$ decreases. To avoid numerical problems, a normalization of the vector $\vec{q}_i$ is performed in each iteration.

The problem appears when there is a λ_j such that $\left|\lambda_j\right| = \left|\lambda_1\right|$.

C. Modified algorithm

To solve this convergence problem, a modification in the original algorithm (expressed in Eq. (4)) has been implemented. To do it, it must be taken into account that the eigenvalues of the matrix *K* of the q-method implemented in ESAT accomplish the following relationships:

$$\begin{aligned} &\lambda_1 = -\lambda_2 \\ &\left|\lambda_1\right| > \left|\lambda_3\right|, \left|\lambda_4\right| \end{aligned} \tag{9}$$

This is why, in our case, if the iteration index is even, the 2ith iteration of the vector $\vec{q}$ can be approached to:

$$\vec{q}_{2i} = \lambda_1^{2i}\left[c_1\vec{x}_1 + c_2\vec{x}_2 + ...\right] \quad , \quad i >> 1 \tag{10}$$

If the iteration index is odd, the $(2i+1)^{th}$ step of the power method returns:

$$\vec{q}_{2i+1} = \lambda_1^{2i+1}\left[c_1\vec{x}_1 - c_2\vec{x}_2 + ...\right] \quad , \quad i >> 1 \tag{11}$$

In fact, this happens when the q-method implemented with magnetometer and accelerometer measurements is solved in ESAT via the power method. This behavior is shown in Fig. 4

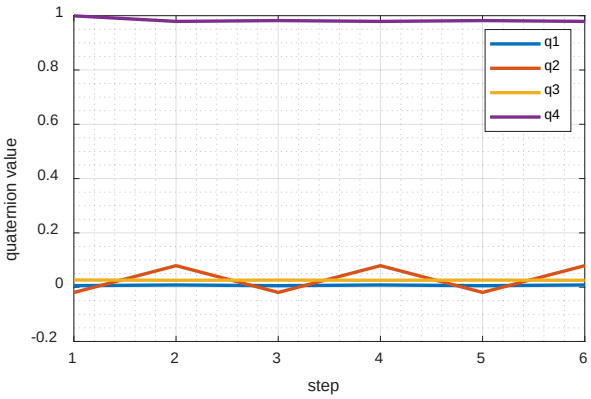

Figure 4. Quaternion value evolution in each iteration of power method (experimental result)

As it is shown in Fig. 4, the quaternion do not converge because of the properties of the eigenvalues of the matrix *K* of the q-method. To solve this problem, when the quaternion does not converge, a new approach to the optimal solution has been developed. It can be obtained with the sum of the Eq. (10) and Eq. (11):

$$\vec{q}_{2i+2} = \frac{\vec{q}_{2i+1} + \vec{q}_{2i}}{2} \approx \lambda_1^{2i+1} c_1 \vec{x}_1 \tag{12}$$

As the other two eigenvalues are smaller than the first (Eq. (9)), if Eq. (12) is applied when this behavior is detected, the modified power method converges to the exact solution. The algorithm that performs this detection and that was finally implemented in ESAT is shown in Fig. 5. The converge criteria is the Euclidean norm of the vector difference between two consecutive iterations. When this value is smaller than a defined tolerance (tol 1) the quaternion is considered to have converged, so, this is the output of the power method and the algorithm finishes. When the vector difference is the same with the opposite sign (oscillating behavior), the norm difference is closed to zero (smaller than another tolerance, tol2) and this is the manner of evaluating the converge.

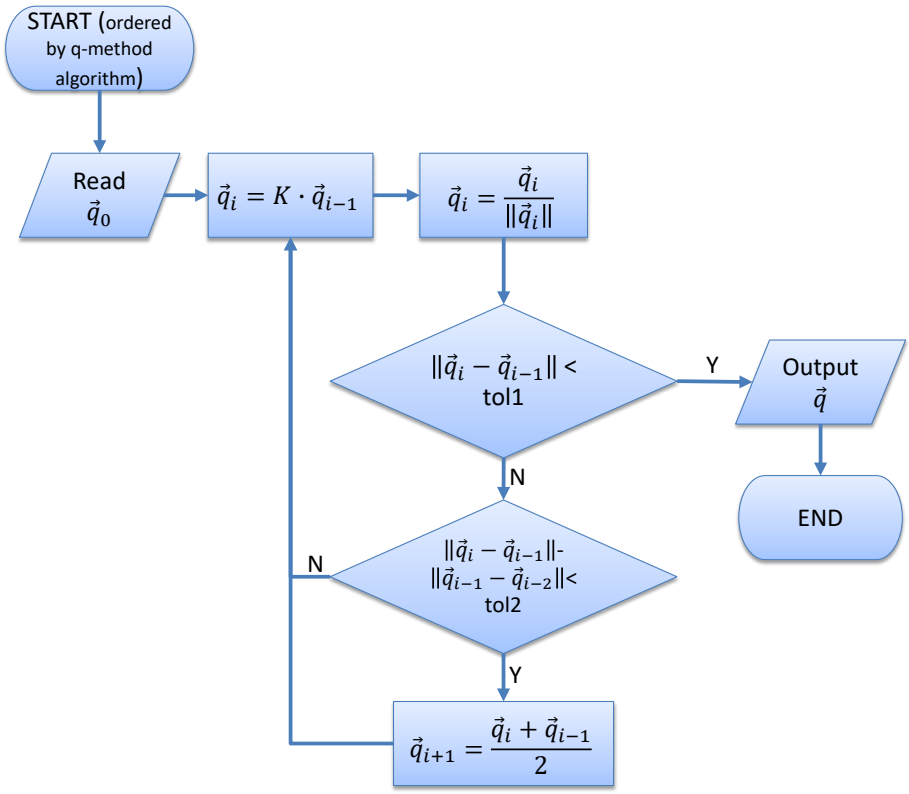

Figure 5. Modified power method final implementation

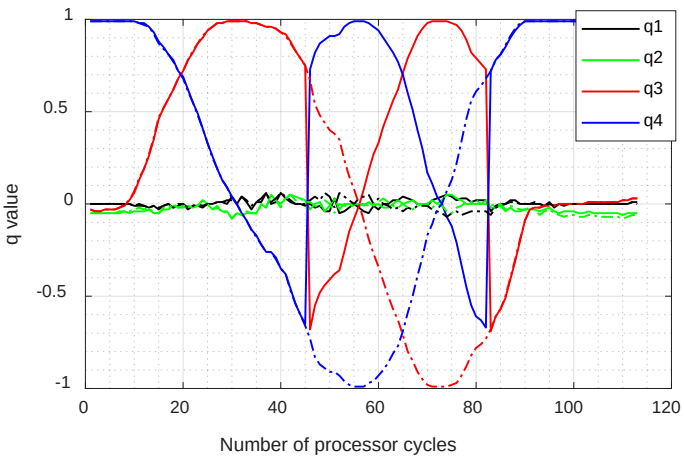

Figure 6. Quaternions obtained on board ESAT with TRIAD method (solid lines) and q-method (dash dot lines)

D. Comparison between q-method and TRIAD method

The last implementation of q-method can be compared with the determination obtained with TRIAD method. To do it, a test consisting on a four radian rotation about z-axis (see Fig. 2) was performed. The determination obtained in this test with the q-method and the TRIAD method (both with accelerometer and magnetometer inputs) is shown in Fig. 6.

It is clear that, as TRIAD is a deterministic method, the same input returns the same output, nevertheless the q-method output depends on the first approach of the solution ($\vec{q}_0$). In this test, this initial approach is the last attitude known (the one obtained in the previous on board processor cycle).

The numerical values are not the same but both methods determine attitude correctly. This is due to the fact that the quaternion $\vec{q}$ expresses the same attitude as $-\vec{q}$ (a rotation δ around a vector $\vec{v}$ is the same as a rotation

$-\delta$ around a vector $-\vec{\upsilon}$). The attitude quaternion is usually defined with $q_4 > 0$ but *the implemented control algorithm does not depend on neither the sign of the current attitude quaternion nor the sign the commanded quaternion (the target attitude).*

It has been empirically probed that this algorithm is very fast, allowing the implementation of the q-method with its eigenvector problem but avoiding the necessity of solving a linear system at each step, which is a common requisite of many eigenvalues algorithms (all which are based in the inverse method). For this reason, this algorithm is able to solving the q-method problem without assuming any simplification (as QUEST method do) even in limited processors).

IV. Actuators

ESAT use three magnetorquers to control its attitude. A magnetorquer actuating in a magnetic field generates a torque according to:

$$\vec{T} = \vec{m} \times \vec{B} \tag{13}$$

Where *T* is the torque generated by the magnetorquer, *B* is the external magnetic field and *m* is the magnetic dipole moment generated by the magnetorquer. The control variable is *m* and it depends on:

$$\left\|\vec{m}\right\| = nIAG \tag{14}$$

Where *n* is the number of coils, *I* is the electrical current trespassing trough the wire, *A* is the area of the coils and *G* is a factor which represent the contribution of the ferromagnetic nucleus of the magnetorquer (in case it exits, if the magnetorquer does not have any nucleus this factor is equal to 1). *G* only depends on the geometry and on the magnetic permeability of the nucleus. For this reason, control *m* is the same as control *I*. To do that, magnetorquers in ESAT are connected to the power bus via H-bridges which are able to produce a PWM output.

V. Control laws

To control the attitude of ESAT, a 3D PID controller has been implemented [7,8]. Next, the control laws are described.

A. Error definition

First of all, a measurement of the difference between the current attitude and the target attitude is necessary (see Fig. 1). The error is a vector in the axis where a torque acting around it can turn the satellite from its current attitude to the target attitude. The magnitude of the error vectors depends on the distance between the two attitudes.

The quaternion error three-dimensional vector, $\vec{q}_\varepsilon$, is the vector part of the four-dimensional quaternion error, q_e, multiplied by the sign of the real part of it:

$$\vec{q}_\varepsilon = \frac{q_4}{|q_4|} q_e \tag{15}$$

The quaternion error, $\vec{q}_e$, is computed as the quaternion multiplication ($\otimes$) of the inverse of the current quaternion, $\vec{q}$, and the commanded quaternion, $\vec{q}_T$ (target) [9,10]:

$$\vec{q}_e = \vec{q}^{-1} \otimes \vec{q}_T \tag{16}$$

Quaternion multiplication, inverse and conjugate are defined as:

$$\vec{q}_a \otimes \vec{q}_b = \begin{bmatrix} q \\ q_4 \end{bmatrix} = \begin{bmatrix} q_{4a}q_b + q_{4b}q_a + q_a \times q_b \\ q_{4a}q_{4b} - q_a \cdot q_b \end{bmatrix} \tag{17}$$

$$\vec{q}^{-1} = \frac{\vec{q}^*}{\left\|\vec{q}^*\right\|} \quad , \quad \vec{q}^* = \begin{bmatrix} -q \\ q_4 \end{bmatrix} \tag{18}$$

All of these operations avoid problems with quaternion signs because if the absolute value of the error angle is lower than 180º, the fourth element of the quaternion error is positive. So, sign changes performed in Eq. (15), assure that the control signal acts in the direction of the shortest way between the target quaternion and the current quaternion. *This means that the control law will function correctly independently of the sign of the estimated quaternion and the commanded quaternion. The only quaternion which must have its real part positive defined is the error quaternion*.

B. PID control law

Due to the wide use of PID controllers and keeping in mind the educational purpose of ESAT, the pointing control law implemented is a 3-axis PID controller. Such a controller is composed by three contributions: proportional, derivative and integral.

Looking at Eq. (13), it is not possible to generate a torque parallel to the external magnetic field which is the one generate by the magnetic field simulator included in ESAT ground equipment. As the control variable is *m*, it has no sense to produce a magnetic dipole moment with a component in the external magnetic axis because it will consume power without generating any torque. In order to get only a contribution in the plane perpendicular to the external magnetic field $\vec{B}$, all the terms of the PID controller are multiplied in a vector product by the external magnetic field versor. So, the implemented magnetic PID controller is:

$$\vec{m} = K_p\left(\vec{B} \times \vec{q}_\varepsilon\right) + K_D\left(\vec{\omega} \times \vec{B}\right) + K_I\left(\vec{B} \times \int \vec{q}_\varepsilon dt\right) \tag{19}$$

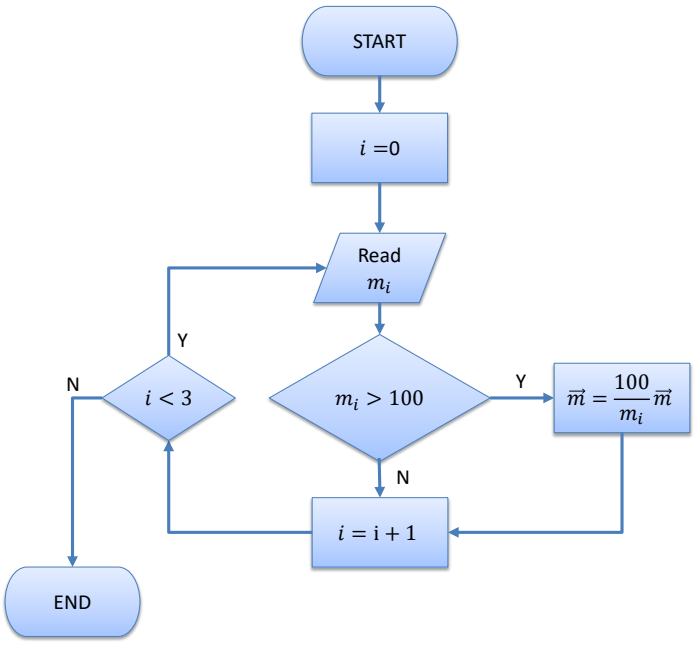

Figure 7. Anti-Windup algorithm

The derivative term of the PID is directly implemented with angular velocity (measured with the gyroscopes). As it has been explained, these signals are filtered so, it is not necessary to include another filter stage in the controller. With respect to the integral term, an anti-windup step has been included. The objective of this step is to prevent the processor from commanding the magnetorquers above the 100% duty cycle *and also to maintain the dipolar moment perpendicular to the external magnetic field*. This last requirement avoids power consumption in the magnetorquers without producing torques. The anti-windup checks if there is one component with a duty cycle larger than 100%. Then, all the components are scaled in order to get the largest component equal to 100%. Anti-Windup algorithm is represented in Fig. 7†.

† Note than C++ zero-based indexes are used in this algorithm.

C. Detumbling

Detumbling consists of damping the angular velocity of the satellite to zero. "When the spacecraft is deployed from the launch vehicle, this process may impart a large angular momentum to the spacecraft, causing the spacecraft to tumble. For the spacecraft to perform meaningful pointing tasks, it must first stop this tumbling motion" [9]. A typical algorithm for LEO orbits is the B-dot control law. This consists on the application of a magnetic dipole moment in the opposite direction of the derivative of the magnetic field vector:

$$\vec{m}_{Bdot} = -k\dot{\vec{B}}_b \tag{20}$$

As the magnetometer is on board, the measurement of the magnetic field vector is expressed in the body frame. Coriolis theorem relates the derivative of the vector:

$$\dot{\vec{B}}_I = \left[\frac{d\vec{B}}{dt}\right]_I = \dot{\vec{B}}_b + \vec{\omega}\times\vec{B} \tag{21}$$

Where the subindex *I* refers to an inertial frame and *b* to body frame. As the magnetic field vector is generated with ESAT magnetic field simulator which is fixed to the inertial frame, its derivative in this frame is zero:

$$\dot{\vec{B}}_I = 0 \Rightarrow \dot{\vec{B}}_b = -\vec{\omega}\times\vec{B} \tag{22}$$

So, the B-dot detumbling algorithm can be expressed as:

$$\vec{m}_{Bdot} = -k\dot{\vec{B}} = k\left(\vec{\omega}\times\vec{B}\right) \tag{23}$$

Which is the same as the derivative part of the PID controller. It means that the same controller can be used to perform a detumbling by simply set proportional and integral gain to zero.

Figure 8. ESAT on the test bed

VI. Ground segment and communications

ESAT communication is establish with the CCSDS space packet protocol.

The ground segment equipment used to perform the validation tests includes a static magnetic field simulator composed by two neodymium magnets, a three-degrees of freedom test bed with a mass balancing system and the ground station able to receive the telemetry packets from ESAT and to send commands. Fig. 8 shows the configuration used in the tests.

VII. Results

A. PID control law

To verify the behavior of this controller, a manoeuvre consisting of a rotation of approximately 165º around Z-axis (see Fig. 3) is commanded with different gains.

Figure 9 and Fig. 10 show the response of the system (satellite + movable part of the test bed) to this command when a P and PD controllers are respectively used with the same proportional gain.

As it is shown in Fig. 10, the derivative gain allows to reduce the oscillating behavior by increasing the damping ratio. The use of the measurements of the gyroscope instead of differentiate the estimated quaternion seems to be a good idea due to the fact that finite differences do not work well with noisy signals because high frequency noise

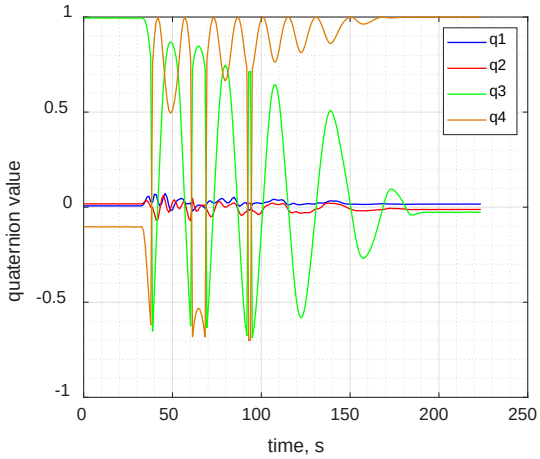

Figure 9. Quaternion output for the validation test with P control

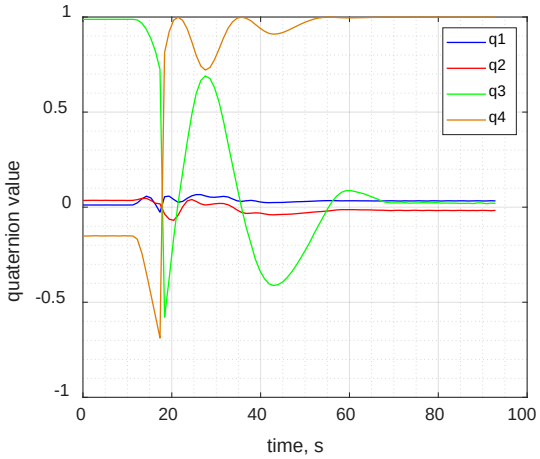

Figure 10.Quaternion output for the validation test with PD control

increases (in both signs) the local derivative value. To avoid this problem, it is usually used a low pass filter in the derivative part of the PID (or PD) controller. Nevertheless, as the signals come from sensors have already been treated, the estimate quaternion seems to be a very "clean" signal able to be differentiated without any more filter. Figure 9 and Fig. 10 illustrate this idea.

This test also shows that the algorithm used do not have problem with the location of the quaternion sign, i.e. no matter if the sign is in the real or in the vector part of the quaternion (as it has been previously mentioned) the controller converges to the command attitude (if the gains do not make the system unstable).

To avoid the apparition of a stationary error due to the fact that when the error is too small, the low commanded signal is less than the one necessary to initialize the movement, the integral part can be added to the controller. It has been also tested and verified. The integral part of the controller is able to drive the system to the commanded state even with the simply Euler algorithm (necessary to compute the integral).

B. Detumbling

To check the behavior of the detumbling algorithm an initial angular velocity is given to satellite. In order to see the difference between the velocity decrement due to the external friction torques and the one produced with the magnetorquers, the algorithm is activated about 40 seconds after the initial impulse. Figure 11 shows this test and how the angular velocity is damped from -100 º/s to 0 in 20 s.

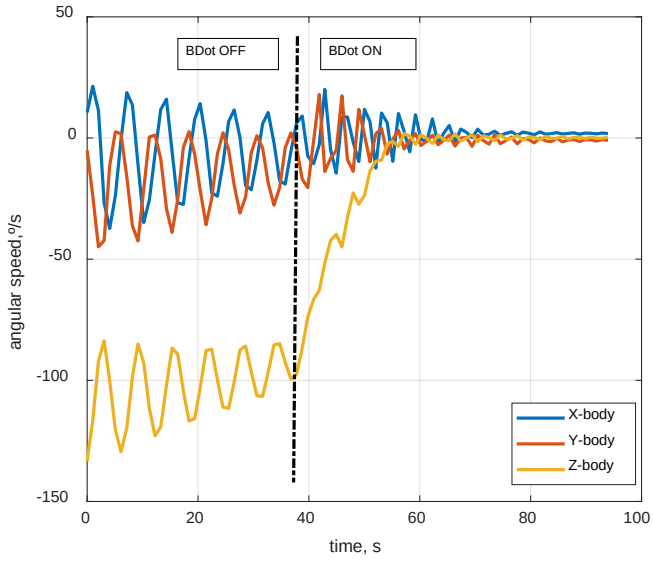

Figure 11. Angular speed evolution with the Bdot detumbling algorithm

VIII. Conclusions

The work described in this document presents a complete ADCS for the educational satellite ESAT, which is now a powerful experimental tool able to support more researches and developments in the field of satellites attitude control. It is currently being used to test the functionality of intelligent systems, like fuzzy controllers, and robust control systems, with H_∞ based methods.

References

[1] A. Mehrparvar, CubeSat Design Specification. Rev 13. The cubesat Program, Cal Poly SLO, 2/20/14.

[2] Theia Space, ESAT brochure., Available in: http://www.theiaspace.com/ products/.

[3] D. Calvo, T. Avilés, V. Lapuerta & A. Laverón-Simavilla, «Fuzzy attitude control for a nanosatellite in low Earth orbit,» *Elsevier*, vol. Expert Systems With Applications, 2016.

[4] K. Grossekatthöfer & Y. Zizung, Introduction into quaternions for spacecraft attitude representation, Berlin, Germany: Technical University of Berlin, Department of Astronautics, May 31, 2012.

[5] J. Diebel, Representing Attitude: Euler Angles, Unit Quaternions, and Rotation Vectors, Standford, California 94301-9010: Standford University, 20 October 2006.

[6] J. Lambers, The Eigenvalue Problem: Power Iterations, Lecture 14 Notes, Summer Sesions 2009-10.

[7] M. J. Sidi, Spacecraft Dynamics and Control. A Practical Engineering Approach, Israel Aircraft Industries Ltd. and Tel Aviv University.

[8] K. Aström & R. Murray, Feedback Systems: An Introduction for Scientist and Engineers, Princeton and Oxford.: Princeton University Press, 2016.

[9] C. Pong, High-Precision Pointing and Attitude Estimation and Control Algorithms for Hardware-Constrained Spacecraft., Massachusetts Institute of technology, Department of Aeronautics and Astronautics, June 2014.

[10] B. Bacon, Quaternion-Based Control Arquitecture for Determining Controllability/Maneuverability Limits, Hampton, VA. 23681: NASA Langley Research Center.